Talanta 230 (2021) 122158

Contents lists available at ScienceDirect

Talanta

journal homepage: www.elsevier.com/locate/talanta

One-step enzyme-free detection of the miRNA let-7a via twin-stage signal amplification

Jiamei Pu [a,1], Mingbin Liu [a,1], Hongbo Li [a,*], Zhigang Liao [d], Weihua Zhao [a], Suqin Wang [a], Yun Zhang [b,**], Ruqin Yu [c,***]

[a] Key Laboratory of Functional Small Organic Molecule, Ministry of Education, College of Chemistry and Chemical Engineering, Jiangxi Normal University, Nanchang, 330022, PR China
[b] College of Chemistry and Bioengineering, Guilin University of Technology, Guilin, 541004, PR China
[c] State Key Laboratory for Chemo/Biosensing and Chemometrics, Hunan University, Changsha, 410082, PR China
[d] Jiangxi Normal University, PR China

ARTICLE INFO

Keywords:
One-step strategy
Twin-stage signal amplification
Enzyme-free detection
miRNA let-7a

ABSTRACT

MicroRNAs (miRNAs) play a significant role in diverse biological processes. The abnormal expression of miRNAs is related to the development of cancers and various diseases. It is of great importance to sensitively and accurately detect miRNAs for early disease diagnosis and treatment. Here, a new fluorescence strategy was initially proposed for the enzyme-free sensing of let-7a by combining the strand displacement reaction (SDR) with the hybridization chain reaction (HCR). The sensor was successfully applied to the detection of the let-7a gene with a wide linear range from 25 pM to 250 nM and a limit of detection (LOD) of 9.01 pM. The fluorescence intensity has a good linear relationship with the logarithm of the target concentration. In addition, the biosensor allowed for the highly sensitive detection of the target genes even in complex human serum samples. With simple operation yet improved detection capability for let-7a, the developed fluorescent biosensor thus shows great potential for early clinical diagnosis as well as biological research.

1. Introduction

Liquid biopsy is based on the analysis of tumor-specific markers in blood samples and provides great help in the diagnosis and guidance of cancer treatment. Liquid biopsy has the advantages of easy sampling, noninvasiveness, simplicity, and provision of molecular information [1,2]. Liquid biopsy originates from the analysis of circulating tumor cells (CTCs). In the clinic, research on circulating tumor DNA (ctDNA) and circulating tumor RNA (ctRNA, including microRNA) has also attracted increasing attention [3,4]. MicroRNAs (miRNAs) are endogenous, short, noncoding RNAs of approximately 18–22 nucleotides that play a significant role in different physiological processes [5,6]. For example, miRNAs can regulate cell proliferation, differentiation, apoptosis and metabolism [7,8]. Much evidence shows that miRNAs can regulate gene expression and can be tumor suppressors or oncogenes [9]. The expression of miRNAs is related to many diseases and cancers. For example, miRNA concentration changes are related to the occurrence and development of cardiovascular diseases, neurodegenerative diseases, autoimmune diseases and various types of cancers [10]. MiRNAs have been used as biomarkers in the early diagnosis of diseases (especially cancers) [11].

Let-7 miRNA was first discovered in *Caenorhabditis elegans* and acts as a time regulator of cell development. The let-7 miRNA family has 12 members (from let-7a to let-7i). Among them, let-7a is being studied in depth because of its large research potential and representativeness [12]. Let-7a is one of the crucial tumor suppressors [13] and an important disease marker [14]. Abnormal expression of let-7a causes a variety of cancers [15]. The low expression of let-7a is related to poor differentiation of normal cells and can lead to the development of aggressive cancers, such as prostate cancer [16], gastric cancer [17]and cervical cancer [18].

The accurate detection of the concentrations of certain miRNAs in

* Corresponding author.
** Corresponding author.
*** Corresponding author.
E-mail addresses: lihongbo112@126.com (H. Li), lzg2239444075@163.com (Z. Liao), zy@glut.edu.cn (Y. Zhang), rqyu@hnu.edu.cn (R. Yu).
[1] These authors contributed equally to this work.

https://doi.org/10.1016/j.talanta.2021.122158
Received 22 October 2020; Received in revised form 22 January 2021; Accepted 26 January 2021
Available online 19 February 2021

the body can help us further understand the pathogenesis of certain cancers [19]. However, due to the strong sequence homology, low concentration and easy degradation of miRNAs, they are not easy to detect with high sensitivity [20,21]. For the purpose of improving the detection sensitivity, isothermal amplification technology has been developed and has been demonstrated to be a promising strategy for nucleic acid detection [22]. Isothermal amplification has aroused great interest in the study of miRNAs because of its advantages of fast amplification speed, high detection sensitivity, and accurate detection [9]. Such methods include hybridization chain reaction (HCR) [23–25], rolling circle amplification [26–28], duplex-specific nuclease amplification [29], strand displacement amplification [30,31], loop-mediated isothermal amplification [32] and recombinase polymerase amplification [33]. Moreover, various techniques have been used to realize sensitive measurement of isothermal amplification products, such as fluorescence detection [11], surface-enhanced Raman spectroscopy [34], colorimetric analysis [35], electrochemical measurement [36], chemiluminescence detection [37] and other technologies.

The most commonly used methods for detecting miRNAs are Northern blotting [38,39], RT-PCR [40] and miRNA microarrays [41]. These methods have been successfully applied to detect miRNAs in preliminary clinical applications and basic research [9]. However, they still need to be greatly improved [42]. For instance, Northern blotting is a relatively simple method, but it requires a large amount of total RNA for each assay run, and it is not sensitive enough for analysis of miRNA at low levels [43]. Although RT-PCR has high sensitivity and specificity, this method is relatively complicated because of the need to design special primers and because it involves error-prone enzyme amplification [40]. Additionally, current microarray technology can perform high-throughput measurements but requires a large amount of initial materials and shows limited sensitivity [42,44]. Therefore, it is still of great importance to develop a simple, rapid, and highly sensitive and selective method for detecting miRNAs. Herein, a biosensing method with these features is proposed for the first time for the detection of let-7a based on a novel twin-stage amplification strategy that integrates SDR with HCR. The experimental results show that a detection limit lower than 10 pM was obtained under the optimal conditions, which makes our method one of the most sensitive sensing systems compared with many other representative techniques.

2. Experiment

2.1. Materials and reagents

The oligonucleotides sequence designed of this experiment was adapted from previously reports [45,46]. Oligonucleotides were synthesized by Sangon Biotechnology Co., Ltd. (Shanghai, China), and their sequences are shown in Table 1. All nucleic acid strands were dissolved and diluted with 1 × TE buffer (10 mM Tris, 1 mM EDTA, pH 8.0) to the concentration required for the experiments. NEB buffer 2 (10 × , 100 mM $MgCl_2$, 500 mM NaCl, 10 mM dithiothreitol (DTT), 100 mM Tris-HCl, pH 7.9) and a low-molecular-weight DNA ladder were purchased from New England Biolabs Inc. (Beijing, China). SYBR Green I was ordered from Dingguo Changsheng Biotechnology Co., Ltd. (Beijing, China). SYBR Green II was ordered from Shanghai Acmec Biochemical Co., Ltd. In addition, all chemical reagents were of analytical reagent grade and used without further purification. All solutions used in the experiments were prepared by Milli-Q water (18.4 MΩ).

2.2. Apparatus

Fluorescence measurements were performed on an LS 55 fluorescence spectrometer (PerkinElmer, USA). The excitation wavelength was set to 492 nm, and the fluorescence emission range recorded was from 450 nm to 650 nm. Polyacrylamide gel electrophoresis experiments were carried out with a gel electrophoresis apparatus (Bio-Rad, USA). The applied voltage was set to 90 V, and the electrophoresis time was 90 min. Gel imaging of the polyacrylamide gel obtained in the experiment was performed by a ChemiDoc XRS (Bio-Rad, USA), and the image obtained was processed using imaging software.

2.3. Gel electrophoresis analysis

Twelve percent nondenaturing polyacrylamide gel electrophoresis (PAGE) was used to test the feasibility of the biosensor proposed in our work. To verify that C1 could be released by SDR. We use 1 × NEB buffer 2 to configure the Single-stranded samples of C1, C2, C3 and assistant probe. The formation of the complex of C1, C2 and C3 was based on the incubation of C1, C2 and C3 in 1 × NEB buffer2 at 37 °C for 1 h. C2 was released by adding the target gene to the complex of C1, C2 and C3, and incubating at 37 °C for 1 h. In order to further release C1, the target gene and assistant probe were added to the complex of C1, C2 and C3, and incubated at 37 °C for 1 h. Then, these samples were mixed with 6 × loading buffer and 100 × SYBR GreenII and incubated in the dark for 10 min. Next, the resultant reaction mixture was transferred into gel wells of freshly prepared PAGE gels (12%), and electrophoresis was performed in 0.5 × TBE buffer for 90 min at 90 V. The gel was imaged using a ChemiDoc XRS (Bio-Rad, USA) imaging system.

For analyze HCR, the reaction products mixed with 6 × loading buffer and 100 × SYBR Green I and incubated in the dark for 10 min. Then, the resultant reaction mixture was transferred into gel wells of freshly prepared PAGE gels (12%), and electrophoresis was performed in 0.5 × TBE buffer for 90 min at 90 V. The gel was imaged using a ChemiDoc XRS (Bio-Rad, USA) imaging system.

Table 1
The oligonucleotide sequences used in this study.

Items		Sequence (5′-3′)
Trigger probe	C1	TCTCAAGGATCACCGCATCTCTCAGAGAC
	C2	CCACATACATCATATTCCCTTGAGGTAGTA GGTTGT
	C3	AACTATACAACCTACTACCTCAAGGGGTCTCTGAGAGATGCGG
Assistant probe		CCGCATCTCTCAGAGACCCCTTGAGGTAGTAGGTTGT
HCR probe	H1	TGAGAGATGCGGT-FAM-GATCCTTGAGACTAAGTTCTCAAGGAT-BHQ-CACCGCAT
	H2	TCTCAAGGAT-FAM-CACCGCATCTCTCAATGCGGT-BHQ-GATCCTTGAGAACTTAG
Analytes	Let-7a	UGAGGUAGUAGGUUGUAUAGUU
	Let-7b	UGAGGUAGUAGGUUGUGUGGUU
	Let-7c	UGAGGUAGUAGGUUGUAUGGUU
	miRNA-141	UAACACUGUCUGGUAAAGAUGG
	miRNA-21	UAGCUUAUCAGACUGAUGUUGA

2.4. Fluorescence detection of the microRNA let-7a

The H1 and H2 probes were annealed at 95 °C for 5 min in a metal bath and then cooled to room temperature (~25 °C) to ensure a stable structure before use. Subsequently, 0.6 μL of 10 μM C1, 1 μL of 10 μM C2, 1 μL of 10 μM C3, 2 μL of 10 × NEB buffer 2 (100 mM $MgCl_2$, 500 mM NaCl, 10 mM dithiothreitol (DTT), 100 mM Tris-HCl, pH 7.9) and 12.1 μL of ultrapure water were mixed and incubated at 37 °C for 1 h. Next, 0.8 μL of 10 μM assistant probe and 0.5 μL of the target let-7a at certain concentrations were added to the reaction solution, followed by 1 h incubation at 37 °C. Then, 1 μL of 10 μM H1 and 1 μL of 10 μM H2 were added to the reaction system and incubated at 37 °C for 1 h to allow the HCR to react completely. Finally, 180 μL of ultrapure water was added to the resulting reaction mixture, and then fluorescence measurement was performed.

3. Results and discussion

3.1. Working principle for let-7a gene detection

The detection principle of this new sensing system is illustrated in Scheme 1. As shown in Stage 1, the trigger probe for the SDR has a three-stranded structure consisting of C1, C2 and C3. In the absence of the target DNA, the trigger probe retained its original three-stranded structure, the subsequent HCR reaction could not be carried out, and the fluorescence intensity of the system was very weak. When the target DNA was introduced, the hybridization reaction between the functional domain d of the target sequence and the functional domain d* of C3 occurred to form the intermediate four-stranded structure. As a result, a rapid displacement reaction occurred to allow C2 to be released and the functional domain b* of C3 to be exposed. C3 could bind the assistant probe to trigger the release of C1. At the same time, the target DNA was regenerated and could bind a new trigger probe to start the next round of SDR, resulting in the release of abundant C1. As shown in Stage 2, C1 could cause H1 to be opened through the toehold-mediated SDR. The newly exposed sticky sequence in H1 was hybridized with H2 to expand H2, and the newly released sticky sequence in H2 was hybridized with another H1. This process was repeated to form a nanowire, and the fluorescent group on the nanowire detached from the quenching group, leading to a significant fluorescence recovery that was positively proportional to the concentration of the target gene in the sample.

3.2. Feasibility analysis of the let-7a gene detection system

First, the feasibility of the sensor for let -7a was evaluated. As shown in Fig. 1A, when only H1 and H2 were present, a very low fluorescence signal value could be observed (curve f). However, when C1 was added, a strong fluorescence signal was obtained (curve a). It indicates that C1 was required to trigger HCR. In the presence of the let-7a gene, a similar strong fluorescence signal was also observed (curve b). This was because the target gene could initiate the SDR and make C1 be produced in large quantities. When the target gene was introduced, the target gene could bond with C1. As a result, a rapid displacement reaction occurred to allow C2 to be released and the functional domain b* of C3 to be exposed. C3 could bind the assistant probe to trigger the release of C1. At the same time, the target DNA was regenerated and could bind a new trigger probe to start the next round of SDR, resulting in the release of abundant C1. A large amount of C1 effectively triggers the HCR. When no target existed in the sensing system, a low fluorescence response was obtained (curve c). Therefore, the data prove that C1 was produced from

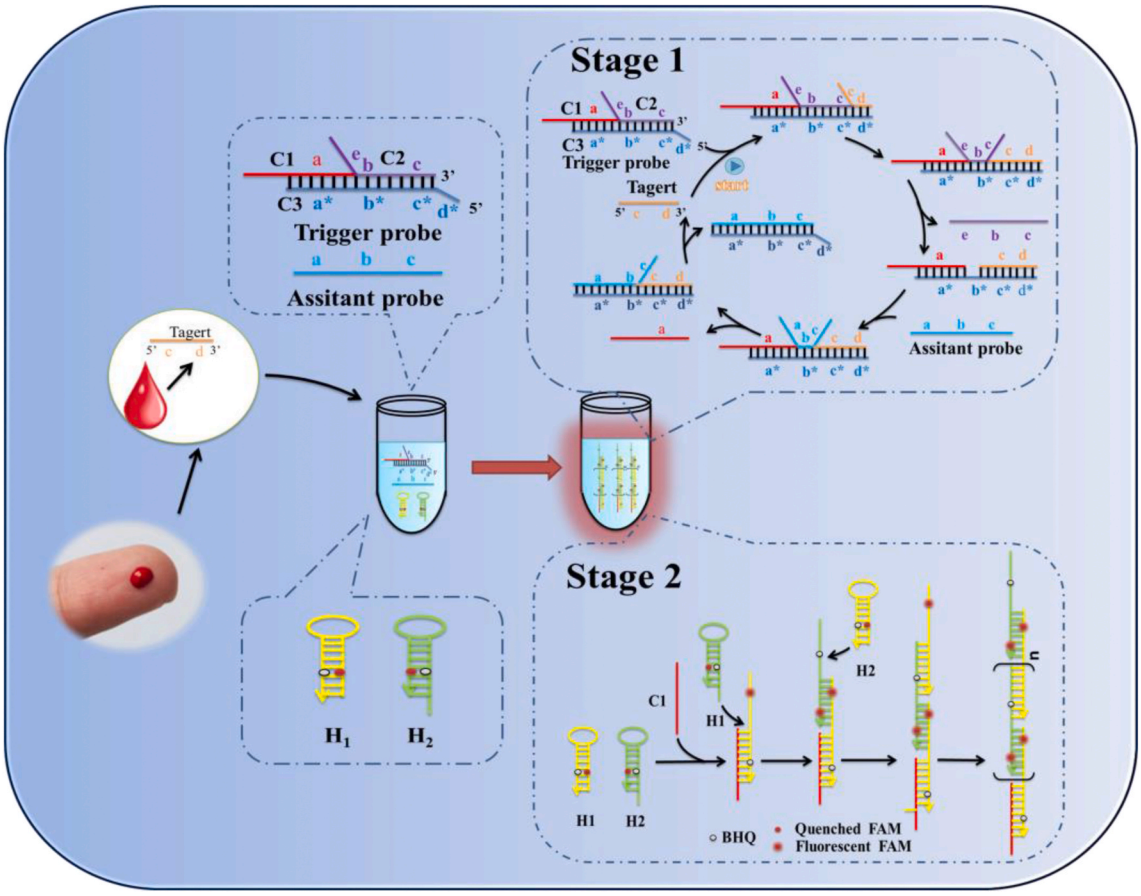

Scheme 1. Stage 1 is schematic diagram of releasing C1 via SDR. The lowercase letters represent the function domains, and function domain x is complementary to function domain x*. Stage 2 is schematic diagram of the HCR triggered by the C1.

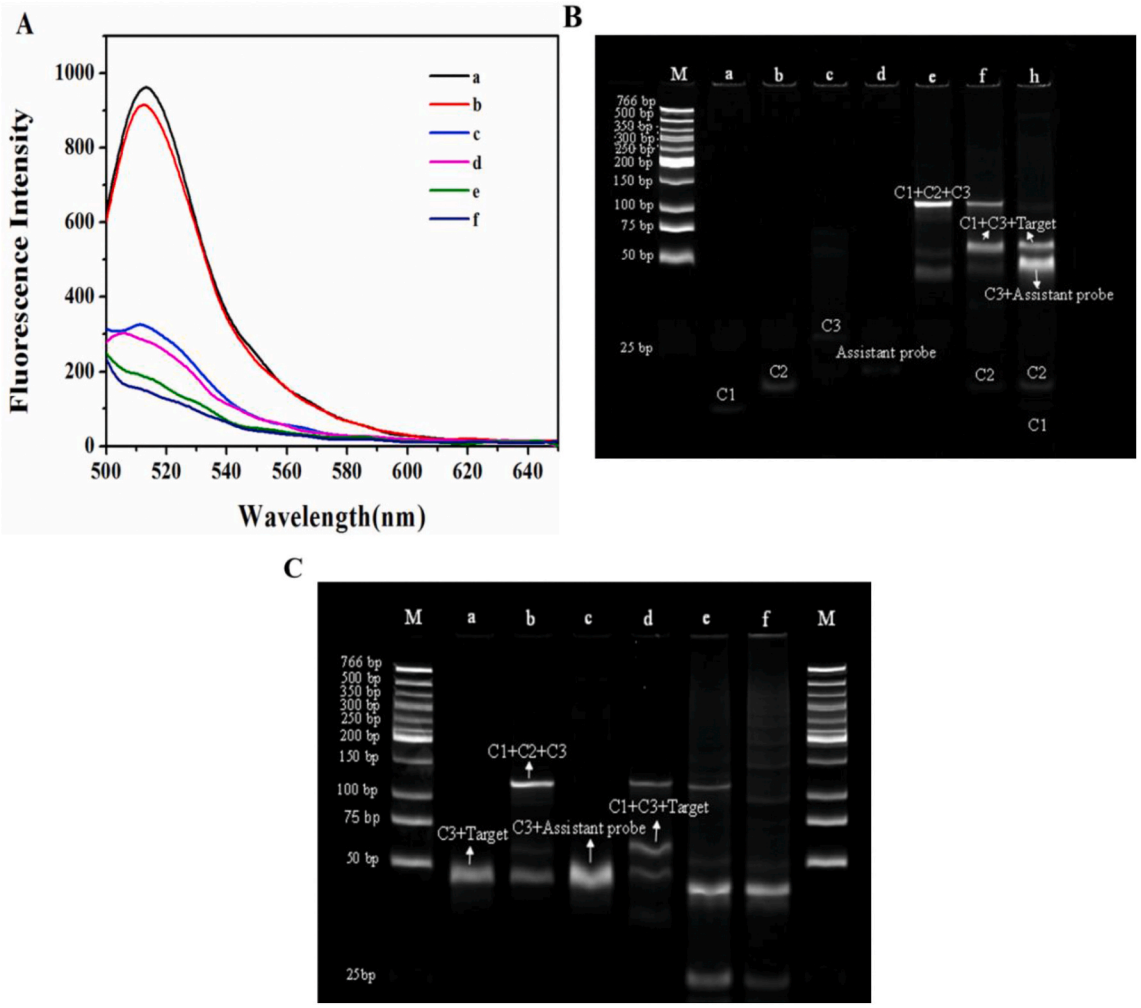

Fig. 1. (A) Fluorescence responses obtained from different mixtures: (a) H1, H2 and C1; (b) C1, C2, C3, H1, H2, target and assistant probe; (c) C1, C2, C3, H1, H2 and assistant probe; (d) C1, C2, C3, H1, H2, target; (e) C2, C3, H1, H2, target and assistant probe; (f) H1 and H2. 12% nondenaturing polyacrylamide gel electrophoresis analysis. (B) M: marker; a: C1; b: C2; c: C3; d: assistant probe; e: C1, C2, C3; f: C1, C2, C3 and target; h: C1, C2, C3, target and assistant probe. (C)M: marker; a: C3 and target; b: C1, C2 and C3; c: C3 and assistant probe; d: C1, C2, C3 and target; e: H1, H2, C1, C2, C3 and assistant probe; f: H1, H2, C1, C2, C3, target and assistant probe. [C1] = 0.3 μM, [C2] = 0.5 μM, [C3] = 0.5 μM, [H1] = 0.5 μM, [H2] = 0.5 μM, [target] = 0.5 μM and [assistant probe] = 0.4 μM.

the SDR in the presence of the target gene (curve b). When there was no C1, a very low fluorescence signal value could be observed (curve e), it proves once again that C1 is indispensable for the occurrence of HCR. When there was no assistant probe, low fluorescence signal can be observed (curve d). After analysis, this is due to the lack of assistant probe, which caused C1 to fail to be released from the trigger probe. When no target existed in the sensing system, a low fluorescence response was obtained (curve c). Therefore, the data prove that C1 was produced from the SDR in the presence of the target gene (curve b). It should be noted that a low fluorescence signal was also obtained from H1 and H2, which may have been caused by a small amount of C1 in the mixture. However, the fluorescence was much lower than that obtained in the case of the target analysis. Highly sensitive detection of let -7a could still be expected by using the proposed sensing system.

Moreover, electrophoresis experiments were also performed to further verify the feasibility of our sensor system. As shown in Fig. 1B , the obvious bands of lanes a-d performed the oligonucleotides of C1, C2, C3 and assistant probe, respectively. When a complex was generated based on the hybridization of C1, C2 and C3, a bright band could be obtained (lane e). In the presence of target gene, it could react with the complex formed by the hybridization of C1, C2 and C3. In this process, C1, C3 and the target formed a new compound, and C2 was released. And then, the hybrid C1, C3 and target could further reacted with assistant probe to the hybrid between assistant probe and C3 with releasing of C1 and target. Therefore, in the lane h, you will see the C1 band, and the released C1 will trigger the step 2 of the HCR. In addition, because the target participates in the cycle, no target band is seen in the lane h.

Fig. 1C shows the gel electrophoresis diagram obtained from different samples. For the samples in lane a and lane c, although they contained different components, their base amounts were similar, so a bright band can be seen at positions with a base amount of 25 bp to 50 bp. Two distinct bands can be seen in lane b. The composition of the sample in lane d had more target sequences than the composition of the sample in lane b. It can be seen that the number of bands in lane d was obviously different from that in lane b, and the bands at positions of 100 bp to 150 bp were also significantly darker than those in lane b because the added target sequence triggered the SDR. The difference between the components contained in lane e and lane f was the addition of the target gene. A weak HCR band can be seen in lane e. This result occurred because when there was no target gene, there was also a small amount of C1 that triggered the HCR. When the target was added, a clear HCR band was observed in lane f, which illustrated the successful construction of the sensor system.

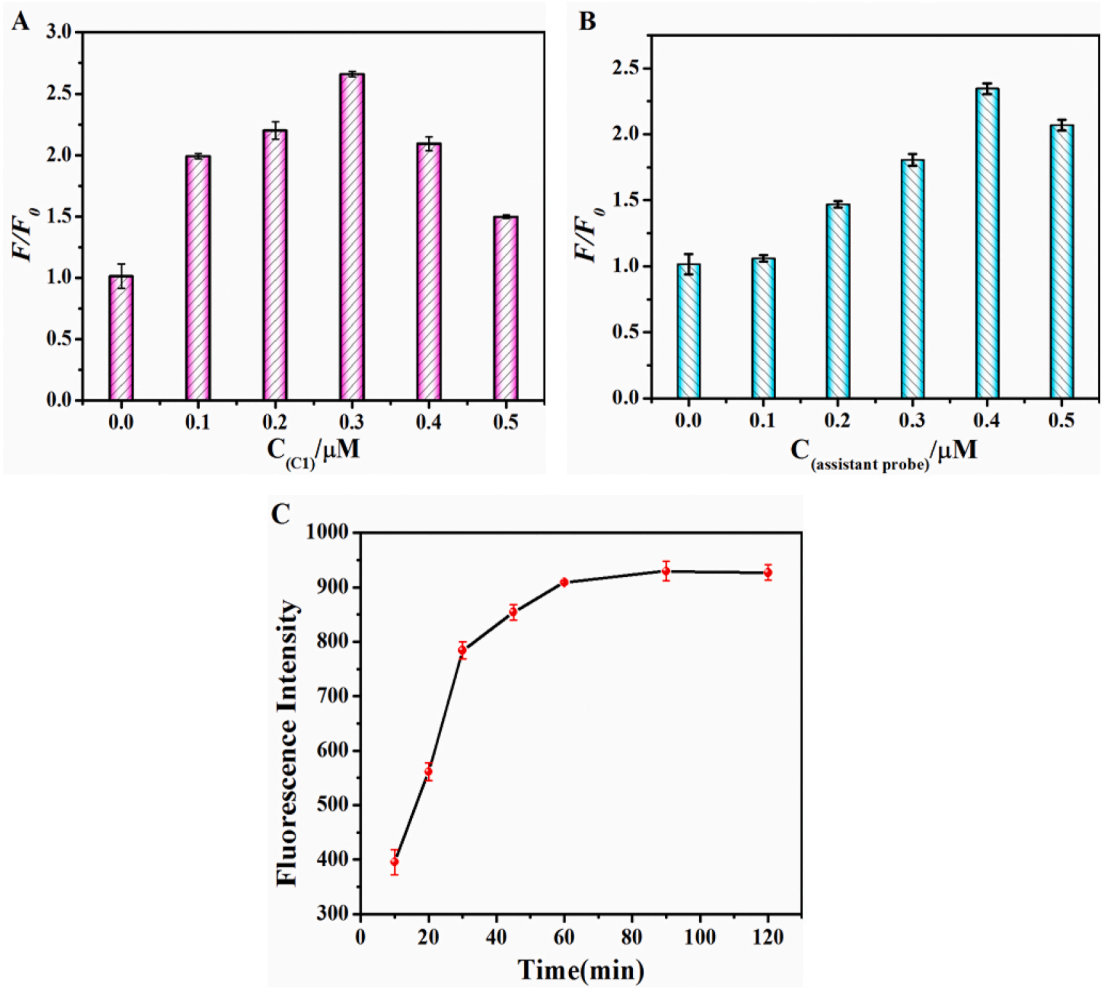

Fig. 2. Effect of (A) C1 concentration, (B) assistant probe concentration, and (C) HCR time on the fluorescence signal of the proposed biosensor. Error bars: SD, n = 3. [H1] = 0.5 μM, [H2] = 0.5 μM, [C2] = 0.5 μM, [C3] = 0.5 μM, [target] = 0.5 μM.

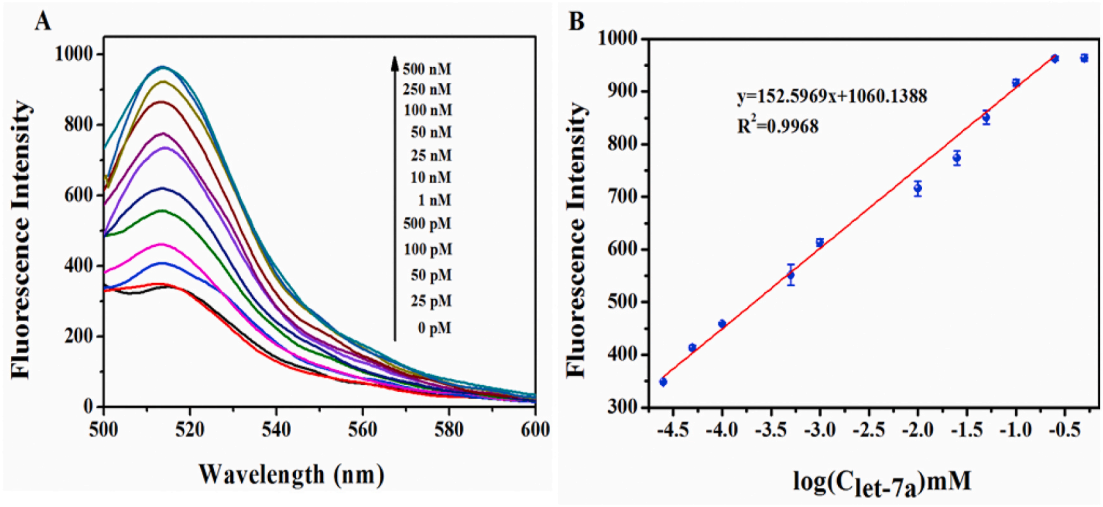

Fig. 3. (A) Fluorescence responses of the biosensor to let-7a at different concentrations in buffer (from bottom to top: 0 pM, 25 pM, 50 pM, 100 pM, 500 pM, 1 nM, 10 nM, 25 nM, 50 nM, 100 nM, 250 nM and 500 nM). (B) Linear relationship between fluorescence intensity and the logarithm of the let-7a concentration. Error bars: SD, n = 3. [C1] = 0.3 μM, [C2] = 0.5 μM, [C3] = 0.5 μM, [H1] = 0.5 μM, [H2] = 0.5 μM, and [assistant probe] = 0.4 μM.

3.3. Optimization of experimental conditions

Before the evaluation of the new biosensor, the main experimental conditions, including the C1 concentration, assistant probe concentration and HCR reaction time, were optimized. The signal-to-noise ratio (F/F_0) was used as the response signal, where F and F_0 are the fluorescence intensity of the reaction system in the presence or absence of the target gene, respectively.

As shown in Fig. 2A, the C1 concentration had a large effect on the response signal of the sensing system. A C1 concentration that is too low or too high will lead to a decrease in the F/F_0 value. This effect is based on the fact that the HCR reaction is not complete in the presence of a C1 concentration that is too low, while the high background fluorescence signal of the system could be produced at a C1 concentration that is too high. The highest F/F_0 value was obtained at the C1 concentration of 0.3 μM, which was therefore used as the optimal concentration in the following experiments.

The concentration of the assistant probe is another important factor that affects the signal amplification of the sensing system. When its concentration is too low, the assistant probe cannot effectively replace C1 to trigger the complete HCR. However, if its concentration is too high, it will also lead to a high background fluorescence signal. As shown in Fig. 2B, as the concentration of the assistant probe increases, the F/F_0 value increases first and then decreases. When the concentration of the assistant probe was 0.4 μM, the F/F_0 value reached its maximum. Therefore, the optimal concentration of the assistant probe was selected to be 0.4 μM.

In addition, the HCR time also directly affects the analytical performance of the sensing system. As shown in Fig. 2C, as the HCR time was increased from 10 min to 60 min, the fluorescence signal (intensity) of the sensing system gradually increased, and no obvious fluorescence increase was observed when the time was prolonged. Therefore, 60 min was chosen as the optimal time for the HCR in all experiments.

3.4. Analytical performance

Under the optimum experimental conditions, the analytical performance of the proposed biosensor for the detection of let-7a in a series of buffer samples was studied. As shown in Fig. 3A, the fluorescence intensity increased steadily as the concentration of let-7a changed from 25 pM to 250 nM. Fig. 3B shows a good linear relationship between the fluorescence intensity and the logarithm of let-7a concentration. The regression equation is $y = 152.5969x + 1060.1388$ ($R^2 = 0.9968$), where y represents the fluorescence intensity value, and x represents the logarithm of the let-7a concentration ($\log(C_{let\text{-}7a})$). The limit of detection (LOD) was calculated to be 9.01 pM, which makes our new method one of the most sensitive miRNA sensing systems compared with many other techniques (Table 2).

Table 2
Comparison of different methods to determine miRNAs.

Analysis method	Detection technique	Linear range	LOD	Reference
Catalyzed Hairpin Assembly	Fluorescence	0.5–50 nM	72 pM	[47]
Double-strand displacement	Fluorescence	5 nM–1000 nM	5.0 nM	[48]
Triplex hybridization chain reaction	Colorimetry	50 pM - 10 nM	27.1 pM	[49]
α-Fe_2O_3 nanoparticle-induced fluorescence quenching	Fluorescence	0.8 nM - 60 nM	0.8 nM	[50]
G-quadruplex-based signal Quenching	Colorimetry	10 nM - 1 μM	4.5 nM	[51]
Hybridization chain reaction	Electrochemistry	30 pM - 7 nM	11 pM	[52]
One-Step Enzyme-Free strategy	Fluorescence	25 pM - 250 nM	9.01pM	This work

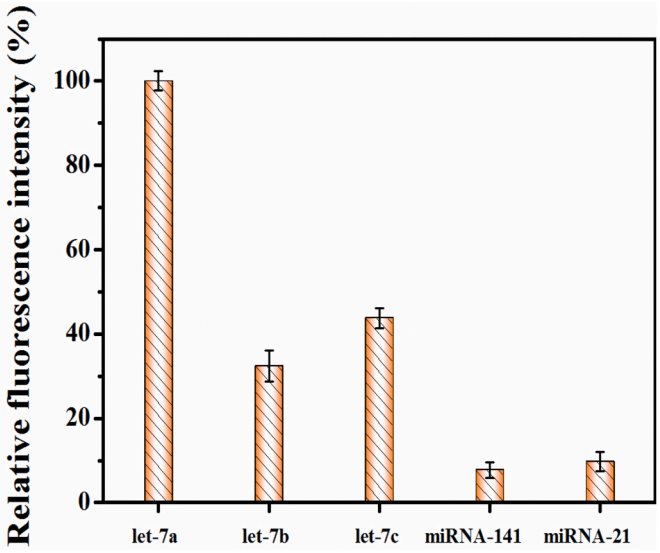

Fig. 4. Selectivity of the Let-7a detection system. [C1] = 0.3 μM, [C2] = 0.5 μM, [C3] = 0.5 μM, [H1] = 0.5 μM, [H2] = 0.5 μM, and [assistant probe] = 0.4 μM. The concentrations of let-7a, let-7b, let-7c, miRNA-141 and miRNA-21 all are 0.5 μM. Error bars: SD, n = 3.

3.5. Specificity

Highly specific analysis of miRNA remains a great challenge because of the high sequence similarity and small size of family members. For instance, the let-7 miRNA family members are highly homologous since their sequence lengths are the same (only 22 bases) and differ by one or two nucleotides. The selectivity of the sensor proposed in this work was investigated by analyzing two homologous miRNAs (let-7b, let-7c) and two kinds of nonhomologous miRNAs (miRNA-141 and miRNA-21) at the same concentration. The relative corresponding fluorescence intensity obtained is presented in Fig. 4. It can be seen that the test sample containing the target let-7a gene produced the highest fluorescence signal. The signals generated by homologous genes (let-7b, let-7c) and nonhomologous genes (miRNA-141 and miRNA-21) were approximately 32%, 44%, 8%, and 10% of those produced from the target gene, respectively. Let-7b and let-7c have the same base length as the target gene let-7a. Let-7b and let-7c differ in length by only two and one base from the target let-7a gene, respectively.

Therefore, let-7b and let-7c can still bind similarly to the target to the trigger probe, causing C1 to be released and triggering the HCR reaction. The difference is that let-7b and let-7c cause C1 to be released to a lesser extent than the target gene. Therefore, the HCR response is weakened to some extent. This is the main reason why let-7b and let-7c show relatively high signals but are still distinguishable from the target let-7a. The base sequences of miRNA-141 and miRNA-21 do not match that of the target; however, due to the high background signal of the control solution, the relative response signal obtained by miRNA-141 and miRNA-21 is relatively high. These results indicate that the proposed miRNA detection method has sequence specificity and can distinguish fully complementary targets from mismatched strands.

3.6. Analysis of human serum samples

To verify the accuracy and practicality of the developed biosensor for let-7a detection, a series of let-7a-spiked diluted (1%) human serum samples were assayed according to general procedures. As shown in Fig. 5, a similar linear detection range from 100 pM to 250 nM was

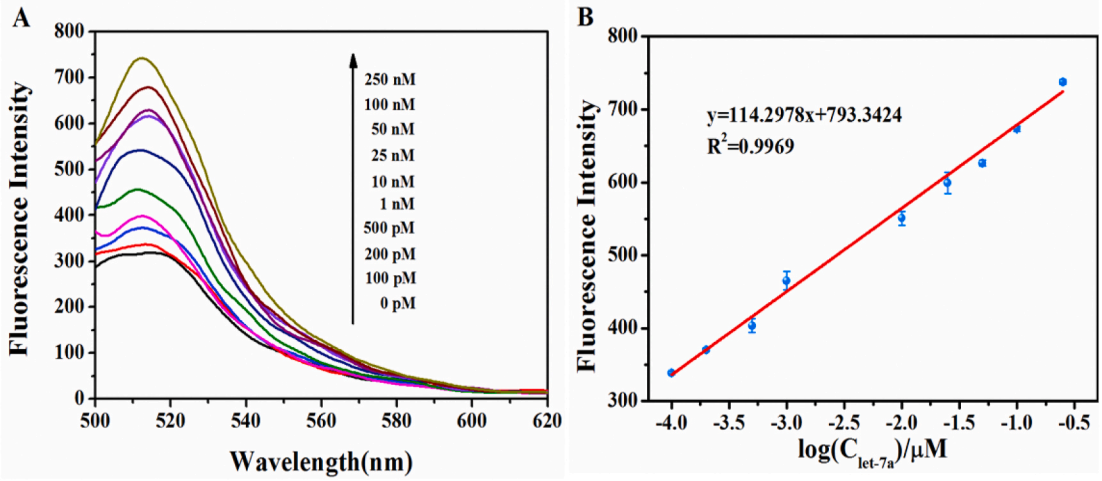

Fig. 5. (A) Fluorescence responses of the sensing system obtained from different concentrations of the target Let-7a in human serum. From bottom to top: 0 pM, 100 pM, 200 pM, 500 pM, 1 nM, 10 nM, 25 nM, 50 nM, 100 nM and 250 nM. (B) Linear relationship between fluorescence intensity and the logarithm of the let-7a gene concentration at a concentration range of 100 pM–250 nM. Error bars: SD, n = 3. [C1] = 0.3 μM, [C2] = 0.5 μM, [C3] = 0.5 μM, [H1] = 0.5 μM, [H2] = 0.5 μM, [target] = 0.5 μM and [assistant probe] = 0.4 μM.

attained, except the fluorescence intensity value recorded for each analyte level was relatively lower than that measured from the corresponding buffer sample, suggesting the good practicality of the new method. Importantly, the data showed that the sensing system maintained its specific molecular recognition ability for the target gene even in real human serum.

4. Conclusions

We successfully developed a novel, enzyme-free biosensor for the amplified fluorescence detection of let-7a via twin-stage amplification based on SDR and HCR. This sensing system offers a wide linear detection range of four orders of magnitude and a LOD as low as 9.01 pM. The fluorescence intensity has a good linear relationship with the logarithm of the target concentration. Moreover, the highly sensitive and specific detection of the target genes, even in complex human serum samples, was also well demonstrated. Because of its simplicity and good sensitivity and selectivity, we believe that this proposed biosensor may hold great potential to be tailored for routine monitoring of target genes of interest in various fields, including clinical diagnosis and biological research.

Author statement

I have made substantial contributions to the conception or design of the work; or the acquisition, analysis, or interpretation of data for the work; AND I have drafted the work or revised it critically for important intellectual content; AND I have approved the final version to be published; AND I agree to be accountable for all aspects of the work in ensuring that questions related to the accuracy or integrity of any part of the work are appropriately investigated and resolved. All persons who have made substantial contributions to the work reported in the manuscript, including those who provided editing and writing assistance but who are not authors, are named in the Acknowledgments section of the manuscript and have given their written permission to be named. If the manuscript does not include Acknowledgments, it is because the authors have not received substantial contributions from nonauthors.

Declaration of competing interest

The authors declare that they have no known competing financial interests or personal relationships that could have appeared to influence the work reported in this paper.

Acknowledgements

This work was supported by National Natural Science Foundation of China (NSFC) (Nos: 21565015, 21663014); Foundation of Jiangxi Educational Committee (No. GJJ150363); State Key Laboratory of Chemical Biosensing & Chemometrics (No. Z2015022); and Key Laboratory of Functional Small Organic Molecules (No. KLFS-KF-201916).

References

[1] J. Das, S.O. Kelley, High-performance nucleic acid sensors for liquid biopsy applications, Angew. Chem. Int. Ed. 59 (2019) 2554–2564.
[2] E. Lianidou, K. Pantel, Liquid biopsies, Gene Chromosome Canc. 58 (4) (2018) 219–232.
[3] C. Bettegowda, M. Sausen, R.J. Leary, I. Kinde, Y. Wang, N. Agrawal, B.R. Bartlett, H. Wang, B. Luber, R.M. Alani, E.S. Antonarakis, N.S. Azad, A. Bardelli, H. Brem, J. L. Cameron, C.C. Lee, L.A. Fecher, G.L. Gallia, P. Gibbs, D. Le, R.L. Giuntoli, M. Goggins, M.D. Hogarty, M. Holdhoff, S.-M. Hong, Y. Jiao, H.H. Juhl, J.J. Kim, G. Siravegna, D.A. Laheru, C. Lauricella, M. Lim, E.J. Lipson, S.K.N. Marie, G. J. Netto, K.S. Oliner, A. Olivi, L. Olsson, G.J. Riggins, S.-B. Andrea, l.-M. Shih, S. M. Oba-Shinjo, S. Siena, D. Theodorescu, J. Tie, T.T. Harkins, S. Veronese, T.-L. Wang, J.D. Weingart, C.L. Wolfgang, L.D. Wood, D. Xing, R.H. Hruban, J. Wu, P. J. Allen, M.S. C, M.A. Choti, V.E. Velculescu, K.W. Kinzler, B. Vogelstein, N. Papadopoulos, L.A. Diaz, Detection of circulating tumor DNA in early- and late-stage human malignancies, Sci. Transl. Med. 6 (224) (2014), 224ra224.
[4] A.M. Newman, S.V. Bratman, J. To, J.F. Wynne, N.C.W. Eclov, L.A. Modlin, C. L. Liu, J.W. Neal, H.A. Wakelee, R.E. Merritt, J.B. Shrager, B.W. Loo, A.A. Alizadeh, M. Diehn, An ultrasensitive method for quantitating circulating tumor DNA with broad patient coverage, Nat. Med. 20 (2014) 548–554.
[5] J. Xu, Z.-S. Wu, Z. Wang, J. Le, T. Zheng, L. Jia, Autonomous assembly of ordered metastable DNA nanoarchitecture and in situ visualizing of intracellular microRNAs, Biomaterials 120 (2016) 57–65.
[6] T. Qi, C. Song, J. He, W. Shen, D. Kong, H. Shi, L. Tan, R. Pan, S. Tang, H.K. Lee, Highly sensitive detection of multiple MicroRNAs by high-performance liquid chromatography coupled with long and short probe-based recycling amplification, Anal. Chem. 92 (7) (2020) 5033–5040.
[7] H. Liu, L. Li, L. Duan, X. Wang, Y. Xie, L. Tong, Q. Wang, B. Tang, High specific and ultrasensitive isothermal detection of microRNA by padlock probe-based exponential rolling circle amplification, Anal. Chem. 85 (16) (2013) 7941–7947.
[8] L.-r. Zhang, G. Zhu, C.-y. Zhang, Homogeneous and label-free detection of microRNAs using bifunctional strand displacement amplification-mediated hyperbranched rolling circle amplification, Anal. Chem. 86 (13) (2014) 6703–6709.
[9] M. Zhou, X. Teng, Y. Li, R. Deng, J. Li, Cascade transcription amplification of RNA aptamer for ultrasensitive MicroRNA detection, Anal. Chem. 91 (8) (2019) 5295–5302.
[10] Z. Shen, L. He, W. Wang, L. Tan, N. Gan, Highly sensitive and simultaneous detection of microRNAs in serum using stir-bar assisted magnetic DNA nanospheres-encoded probes, Biosens. Bioelectron. 148 (2020) 111831.

[11] G.-l. Wang, C.-y. Zhang, Sensitive detection of MicroRNAs with hairpin probe-based circular exponential amplification assay, Anal. Chem. 84 (16) (2012) 7037–7042.
[12] Y. Gao, J. Tian, X. Zhang, B. Qiao, Y. Cao, X. Wang, Q. Wu, A fluorescence assay for microRNA let-7a by a double-stranded DNA modified gold nanoparticle nanoprobe combined with graphene oxide, Analyst 145 (4) (2020) 1190–1194.
[13] S. Roush, F.J. Slack, The let-7 family of microRNAs, Trends Cell Biol. 18 (10) (2008) 505–516.
[14] Y. Li, X. Li, Y. Meng, H. Xu, Photoelectrochemical platform for MicroRNA let-7a detection based on graphdiyne loaded with AuNPs modified electrode coupled with alkaline phosphatase, Biosens. Bioelectron. 130 (2019) 269–275.
[15] D. Qiu, J. Chen, J. Liu, Z. Luo, W. Jiang, J. Huang, Z. Qiu, W. Yue, L. Wu, Expression of microRNA let-7a positively correlates with hepatitis B virus replication in hepatocellular carcinoma tissues, Exp. Biol. Med. 242 (9) (2017) 939–944.
[16] M. Wang, Y. Hu, M.D. Amatangelo, M.E. Stearns, Role of ribosomal protein RPS2 in controlling let-7a expression in human prostate cancer, Mol. Canc. Res. 9 (1) (2011), 1-1.
[17] R. Tang, C. Yang, X. Ma, Y. Wang, D. Luo, C. Huang, Z. Xu, P. Liu, L. Yang, MiR-let-7a inhibits cell proliferation, migration, and invasion by down-regulating PKM2 in gastric cancer, Oncotarget 7 (2016) 5972–5984.
[18] M. Guo, X. Zhao, X. Yuan, J. Jiang, P. Li, MiR-let-7a inhibits cell proliferation, migration, and invasion by down-regulating PKM2 in cervical cancer, Oncotarget 8 (17) (2017) 28226–28236.
[19] A. Esquela-Kerscher, F.J. Slack, Oncomirs — microRNAs with a role in cancer, Nat. Rev. Canc. 6 (2006) 259–269.
[20] T. Tian, J. Wang, X. Zhou, A review: microRNA detection methods, Org. Biomol. Chem. 13 (8) (2014) 2226–2238.
[21] T. Ouyang, Z. Liu, Z. Han, Q. Ge, MicroRNA detection specificity: recent advances and future perspective, Anal. Chem. 91 (5) (2019) 3179–3186.
[22] J. Li, J. Macdonald, Advances in isothermal amplification: novel strategies inspired by biological processes, Biosens. Bioelectron. 64 (2014) 196–211.
[23] X. Feng, H.I. Ming, Triggering hairpin-free chain-branching growth of fluorescent DNA dendrimers for nonlinear hybridization chain reaction, J. Am. Chem. Soc. 136 (28) (2014) 9810–9813.
[24] R.M. Dirks, N.A. Pierce, Triggered amplification by hybridization chain reaction, Proc. Natl. Acad. Sci. U. S. A 101 (43) (2004) 15275–15278.
[25] Y. Zhang, D. Gao, J. Fan, J. Nie, S. Le, W. Zhu, J. Yang, J. Li, Naked-eye quantitative aptamer-based assay on paper device, Biosens. Bioelectron. 78 (2015) 538–546.
[26] R. Deng, L. Tang, Q. Tian, Y. Wang, L. Lin, J. Li, Toehold-initiated rolling circle amplification for visualizing individual MicroRNAs in situ in single cells†, Angew. Chem. 126 (9) (2014) 2421–2425.
[27] R. Deng, K. Zhang, Y. Sun, X. Ren, J. Li, Highly specific imaging of mRNA in single cells by target RNA-initiated rolling circle amplification, Chem. Sci. 8 (5) (2017) 3668–3675.
[28] R. Deng, K. Zhang, L. Wang, X. Ren, M. Sun, J. Li, DNA-Sequence-Encoded rolling circle amplicon for single-cell RNA imaging, Inside Chem. 4 (6) (2018) 1373–1386.
[29] D. Federica, K. Prakash, B. Virgilio, P.P. Pier, F. Roberto, Absolute and direct microRNA quantification using DNA-gold nanoparticle probes, J. Am. Chem. Soc. 136 (6) (2014) 2264–2267.
[30] J.-L. He, Z.-S. Wu, H. Zhou, H.-Q. Wang, J.-H. Jiang, G.-L. Shen, R.-Q. Yu, Fluorescence aptameric sensor for strand displacement amplification detection of cocaine, Anal. Chem. 82 (4) (2010) 1358–1364.
[31] R. Duan, X. Zuo, S. Wang, X. Quan, D. Chen, Z. Chen, L. Jiang, C. Fan, F. Xia, Lab in a tube: ultrasensitive detection of microRNAs at the single-cell level and in breast cancer patients using quadratic isothermal amplification, J. Am. Chem. Soc. 135 (12) (2013) 4604–4607.
[32] T.D. Rane, L. Chen, H.C. Zec, T.-H. Wang, Microfluidic continuous flow digital loop-mediated isothermal amplification (LAMP)†, 00, Lab Chip (2014) 1–3.
[33] S. Lutz, P. Weber, M. Focke, B. Faltin, J. Hoffmann, C. Müller, D. Mark, G. Roth, P. Munday, N. Armes, O. Piepenburg, R. Zengerle, F. von Stetten, Microfluidic lab-on-a-foil for nucleic acid analysis based on isothermal recombinase polymerase amplification (RPA), Lab Chip 10 (7) (2010) 887–893.
[34] L.-P. Ye, J. Hu, L. Li, C.-y. Zhang, Surface-enhanced Raman spectroscopy for simultaneous sensitive detection of multiple microRNAs in lung cancer cells, Chem. Commun. 50 (80) (2014) 11883–11886.
[35] W. Shen, H. Deng, Y. Ren, Z. Gao, A real-time colorimetric assay for label-free detection of microRNAs down to sub-femtomolar levels, Chem. Commun. 49 (43) (2013) 4959–4961.
[36] N. Hao, X.L. Li, H.-R. Zhang, J.-J. Xu, H.-Y. Chen, A highly sensitive ratiometric electrochemiluminescent biosensor for microRNA detection based on cyclic enzyme amplification and resonance energy transfer, Chem. Commun. 50 (94) (2014) 14828–14830.
[37] Q. Wang, B.-C. Yin, Y. Bang-Ce, A novel polydopamine-based chemiluminescence resonance energy transfer method for microRNA detection coupling duplex-specific nuclease-aided target recycling strategy, Biosens. Bioelectron. 80 (2016) 366–372.
[38] A. Valoczi, C. Hornyik, N. Varga, J. Burgyan, S. Kauppinen, Z. Havelda, Sensitive and specific detection of microRNAs by northern blot analysis using LNA-modified oligonucleotide probes, Nucleic Acids Res. 32 (22) (2004) e175.
[39] Y. Zhang, Y. Yan, W. Chen, W. Cheng, S. Li, X. Ding, D. Li, H. Wang, H. Ju, S. Ding, A simple electrochemical biosensor for highly sensitive and specific detection of microRNA based on mismatched catalytic hairpin assembly, Biosens. Bioelectron. 68 (2015) 343–349.
[40] S. Kim, J.-E. Park, W. Hwang, J. Seo, Y.-K. Lee, J.-H. Hwang, J.-M. Nam, Optokinetically encoded nanoprobe-based multiplexing strategy for MicroRNA profiling, J. Am. Chem. Soc. 139 (9) (2017) 3558–3566.
[41] J.M. Lee, Y. Jung, Two-temperature hybridization for microarray detection of label-free MicroRNAs with attomole detection and superior specificity, Angew. Chem. Int. Ed. 50 (2011) 12487–12490.
[42] J.-X. Chen, Y. Zhuo, X. Peng, Y.-Q. Chai, R. Yuan, W.-B. Liang, A dynamic DNA machine via free walker movement on lipid bilayer for ultrasensitive electrochemiluminescent bioassay, Anal. Chem. 91 (21) (2019) 14125–14132.
[43] S. Li, L. Xu, W. Ma, X. Wu, M. Sun, H. Kuang, L. Wang, N.A. Kotov, C. Xu, Dual-mode ultrasensitive quantification of MicroRNA in living cells by chiroplasmonic nanopyramids self-assembled from gold and upconversion nanoparticles, J. Am. Chem. Soc. 138 (1) (2016) 306–312.
[44] D. Li, W. Cheng, Y. Li, Y. Xu, X. Li, Y. Yin, H. Ju, S. Ding, Catalytic hairpin assembly actuated DNA nanotweezer for logic gate building and sensitive enzyme-free biosensing of MicroRNAs, Anal. Chem. 88 (15) (2016) 7500–7506.
[45] F. Ma, S.-h. Wei, C.-y. Zhang, Construction of a robust entropy-driven DNA nanomachine for single-molecule detection of rare cancer cells, Anal. Chem. 91 (12) (2019) 7505–7509.
[46] Z. Wu, G.-Q. Liu, X.-L. Yang, J.-H. Jiang, Electrostatic nucleic acid nanoassembly enables hybridization chain reaction in living cells for ultrasensitive mRNA imaging, J. Am. Chem. Soc. 137 (21) (2015) 6829–6836.
[47] Y. Liu, T. Shen, J. Li, H. Gong, C. Chen, X. Chen, C. Cai, Ratiometric fluorescence sensor for the MicroRNA determination by catalyzed hairpin assembly, ACS Sens. 2 (10) (2017) 1430–1434.
[48] R. Liao, K. He, C. Chen, X. Chen, C. Cai, Double-strand displacement biosensor and quencher-free fluorescence strategy for rapid detection of MicroRNA, Anal. Chem. 88 (8) (2016) 4254–4258.
[49] W. Chen, X. Zhang, J. Li, L. Chen, N. Wang, S. Yu, G. Li, L. Xiong, H. Ju, Colorimetric detection of nucleic acids through triplex-hybridization chain reaction and DNA-controlled growth of platinum nanoparticles on graphene oxide, Anal. Chem. 92 (3) (2020) 2714–2721.
[50] C. Song, G.-Y. Wang, D.-M. Kong, A facile fluorescence method for versatile biomolecular detection based on pristine α-Fe2O3 nanoparticle-induced fluorescence quenching, Biosens. Bioelectron. 68 (2015) 239–244.
[51] L. Lan, R.-L. Wang, L. Liu, L. Cheng, A label-free colorimetric detection of microRNA via G-quadruplex-based signal quenching strategy, Anal. Chim. Acta 1079 (2019) 207–211.
[52] M. Liang, M. Pan, J. Hu, F. Wang, X. Liu, Electrochemical biosensor for MicroRNA detection based on cascade hybridization chain reaction, ChemElectroChem 5 (10) (2018) 1380–1386.